Adhesion Properties of Polyvinyl-Butyral-Laminated Glass under High-Speed Loading

Zhifei Chen [a, c], Xing Chen [a], Suwen Chen [a, b]

a   College of Civil Engineering, Tongji University, Shanghai, China.
b   State Key Laboratory for Disaster Reduction in Civil Engineering, Tongji University, Shanghai, China.
c   China Railway 15th Bureau Group Co., Ltd., Shanghai 200070, China.

Abstract

Laminated glass has been widely used as safety glass for decades owing to its remarkable post-breakage load-bearing capacity. The post-breakage behaviour of laminated glass is mainly affected by several key factors such as the interlayer property, the adhesion property of the glass-interlayer interface, and the size of glass fragments. In this study, the adhesion properties of polyvinyl butyral (PVB) laminated glass under high-speed uniaxial tension were studied by through-cracked tensile (TCT) tests. Two adhesion grades (i.e., BG-R15 medium adhesion grade and BG-R20 high adhesion grade) PVB-laminated glass and three loading rates (i.e., 0.1m/s, 0.5m/s, and 5m/s) were considered in the tests. The delamination behaviour of PVB-laminated glass was modelled using a numerical cohesive zone model (CZM) to accurately calibrate the interfacial adhesion properties. It was found that BG-R15 PVB-laminated glass exhibits a progressive delamination behaviour under high-speed loading, which results in a stable but low post-cracking force, whereas the delamination was significantly constrained for BG-R20 PVB-laminated glass, which leads to a higher post-cracking force but very poor deformability. The deformability of high adhesion grade laminated glass increases with the crack number since more PVB participates into the stretching of cracked laminated glass. The interfacial adhesion property shows a significant rate effect, with the bonding strength and energy release rate of BG-R15 PVB-laminated glass increase by nearly 25% and 50%, respectively, as the loading rate increases from 0.1m/s to 5m/s. In general, the energy dissipation capacity of the BG-R15 PVB-laminated glass is much higher than that of the BG-R20 PVB-laminated glass. This study can provide a valuable reference for the design of laminated glass under blast or impact loads.

Keywords

PVB-laminated glass, Delamination behaviour, TCT test, Adhesion grade, CZM model, Adhesion properties, Rate effect.

Article Information

1. Introduction

Laminated glass is normally composed of glass panes and interlayers. It can retain the glass shards on the interlayer after glass fracture and hence effectively prevents fragment ejections. The post-breakage properties of laminated glass are close related to the mechanical property of interlayer, interfacial adhesion, as well as fracture patterns of the panel (Delincé et al. 2010). Several types of interlayer are commonly used in laminated glass, e.g., polyvinyl butyral (PVB), ionomer, and ethylene vinyl acetate (EVA). Among them, PVB is the most commonly used interlayer for laminated glass (Schuster et al. 2020).

The adhesion between PVB interlayers and glass is formed by the reversible hydrogen links between polyvinyl alcohol in PVB and the silanol groups in the glass under high temperature and high pressure (Schuster et al. 2020). The interfacial adhesion is strongly affected by film composition, e.g., the content of polyvinyl alcohol, the presence of adhesion-regulating additives or the interlayer moisture content (Chen et al. 2022). TCT test (Sha et al. 1997) was conducted to investigate the interfacial adhesion property of PVB-laminated glass. In a TCT test, the uniaxial load is applied on the laminated glass specimen with coincident cracks aligned on the mid-span of both glass panes. The stretching of the interlayer and delamination develop simultaneously under uniaxial tension. A plateau will form on the force-displacement curve when stable delamination occurs, indicating an energy equilibrium is reached between external work and the energy consumption of the interfacial delamination as well as the interlayer strain energy. Based on the obtained force-displacement curves, the interfacial fracture properties can be determined through analytical method or finite element method. For example, Muralidhar et al. (2000) proposed an analytical method to determine the energy release rate based on the energy balance principle, and solutions were given with the PVB treated as an elastic or hyper elastic material. The method was further developed by Butchart and Overend (2012) by considering the viscoelasticity of polymers. On the other hand, cohesive zone models (CZM) were intensively used to simulate the delamination of laminated glass and calibrate the interfacial adhesion parameters for laminated glass (Del Linz et al. 2017, Samieian et al. 2019, Chen et al. 2021a).

From previous studies, it is known that the interfacial adhesion property of PVB-laminated glass is strongly affected by adhesion strength (Sha et al. 1997, Franz et al. 2014), loading rate (Sha et al. 1997, Ferretti et al. 2012, Elzière et al. 2017, Fourton et al. 2020), and environmental conditions (Samieian et al.2018, Samieian et al. 2019, Yang et al. 2022). In this study, a series of TCT tests were conducted to systematically investigate the adhesion properties of PVB-laminated glass under high loading rates. Different adhesion grades (BG-R15 and BG-R20), loading rates (0.1m/s, 0.5m/s, and 5m/s), and fracture patterns (single crack and evenly distributed cracks) were considered. Digital image correlation (DIC) technology was employed to trace the deformation and delamination length of the specimens. Based on the test results, the energy release rate was determined through a 2D plane strain numerical cohesive zone model. The results show that the adhesion grade strongly affect the delamination performance of laminated glass. Compared with the BG-R20 PVB-laminated glass, the BG-R15 PVB-

laminated glass exhibits superior deformability and energy consumption capacity when subjected to high-speed loading. Both the bonding strength and energy release rate increase with the loading rate. The increase of crack numbers can significantly improve the delamination and deformability of BG-R20 PVB-laminated glass. This study can offer a reference for practical design of laminated glass component under blast/impact loads.

2. PVB properties

The PVB interlayers adopted in the tests are TROSIFOL® BG series PVB from Kuraray (2017a, 2017b, 2017c). Three adhesion grades were classified, i.e., BG-R10 (low adhesion), BG-R15 (medium adhesion), and BG-R20 (high adhesion). According to the information from the manufacturer, the mechanical properties of PVBs with different adhesion level are nearly identical. Therefore, uniaxial tensile tests were performed only on BG-R20 to characterize its tensile properties under different strain rates. According to ISO-37 standard (2017), type 1A specimen was selected, and the geometry of specimen is shown in Figure 1a. The nominal thickness of PVB is 1.52mm. The preset loading rates of the test are 0.05m/s, 0.5m/s, and 5m/s, which corresponds to designed strain rates of 1 /s, 10 /s, and 100 /s. Three repeated tests were conducted for each strain rate.

The tests were performed on an Instron testing machine (Figure 1b). A gripper (Figure 1c) was designed to fulfil the acceleration requirement of high-speed loading. The force was recorded by a load sensor mounted on the bottom of the machine with a maximum loading of 100kN, and the accuracy is 0.001kN. The test temperature was 22 ± 2°C, and the humidity was 35 ± 5%.

DIC technology was adopted to record the deformation of the interlayer. The surface of the specimen was pre-coated with random speckles. The strain distribution on the PVB was obtained through VIC-2D software with an error of less than 10 micro strains (VIC-2D 2021). The deformation process and strain distribution for 10/s strain rate are given in Figure 1d. The strain distribution in the gauge section is uniform. The engineering stress was obtained by the dividing the load with the sectional area of the gauge section. Low-pass filtering and smoothing technique was used to reduce the influence of high-frequency oscillation on the stress results. The final engineering stress-elongation (σ_0-λ) curves of PVB are shown in Figure 1e, where $\lambda = 1 + \varepsilon_0$, and ε_0 is the engineering strain. The average strain rate for each testing case is given in Figure 1e. The strain rate effect of PVB interlayer is obvious when the strain rate increases from 1.8/s to 120/s. Good consistency can be observed for repeated tests.

(a) PVB specimen profile (Unit: mm) (b) INSTRON VHS160/100-20 (c) Material gripper

(d) Strain distribution of PVB (10/s) (e) Engineering stress- elongation curves of PVB
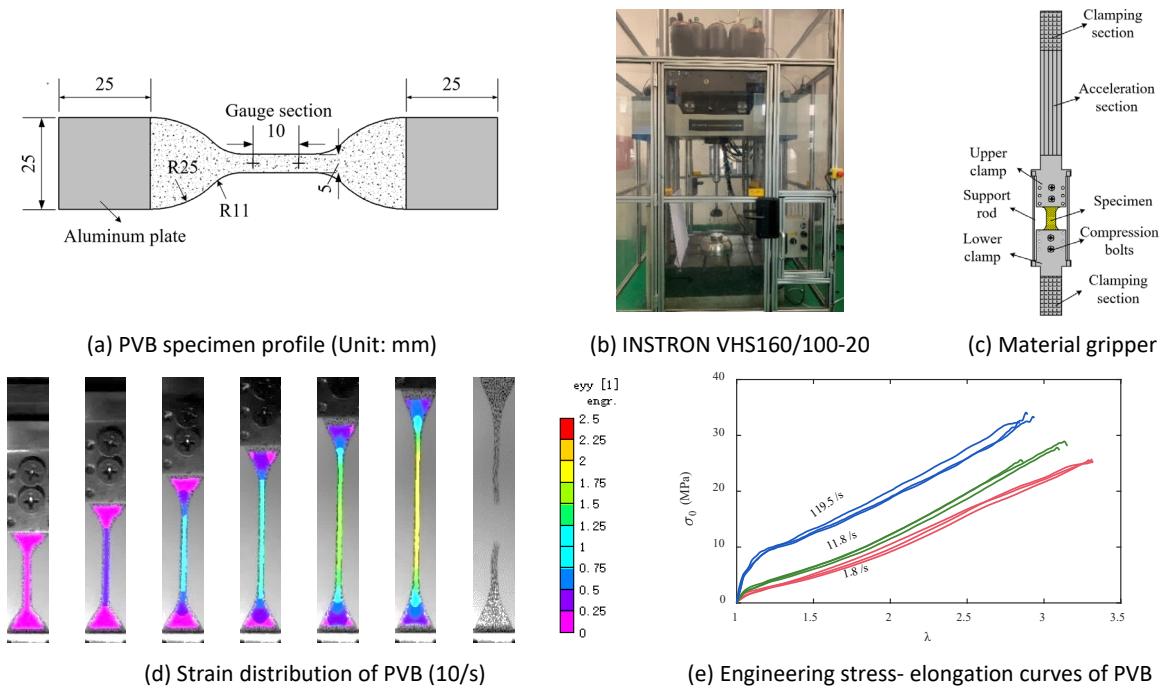
Fig. 1: Material test.

3.   TCT Tests

3.1.   Test conditions and setup

The laminated glass specimens used in this test were manufactured by Tianjin North Glass®. The dimension of the specimen was 200×50 mm, with a configuration of two 4 mm float glass panes and one 1.52 mm (BG-R15 or BG-R20) PVB interlayer. To avoid slipping during the test, aluminium sheets (0.5 mm thick) were bonded to the clamping ends. Two crack patterns, i.e., single crack (Figure 2a) and five uniform distributed cracks (Figure 2b) were considered. The glass panes were pre-damaged along the longitudinal central lines on both sides with a glass cutter and then carefully broken with a four-point-bending device. Three loading rates, i.e., 0.1m/s, 0.5m/s, and 5m/s, were designed to investigate the influence of loading rate on the delamination properties of cracked PVB-laminated glass. The test temperature was 22 ± 2°C, and the humidity was 35 ± 5%, which are the same with that of the uniaxial tensile tests of PVB interlayer.

The test layout is shown in Figure 2c, and the loading process can be seen in Figure 2d. Two high-speed cameras were adopted to capture the deformation from front and side (Figure 3e). Figure 2f shows the delamination front of the specimen, in which δ is the relative displacement at both ends of the specimen, and a_1 and a_2 are the delamination lengths of the lower and upper panels, respectively. The displacement was obtained by the DIC analysis, and the delamination length is the average delamination length of the five evenly distributed points on the delamination front.

(a) Single crack	(b) Uniform crack	(c) Test layout

(d) Loading process	(e) Glass gripper and DIC set-up	(f) DIC analysis
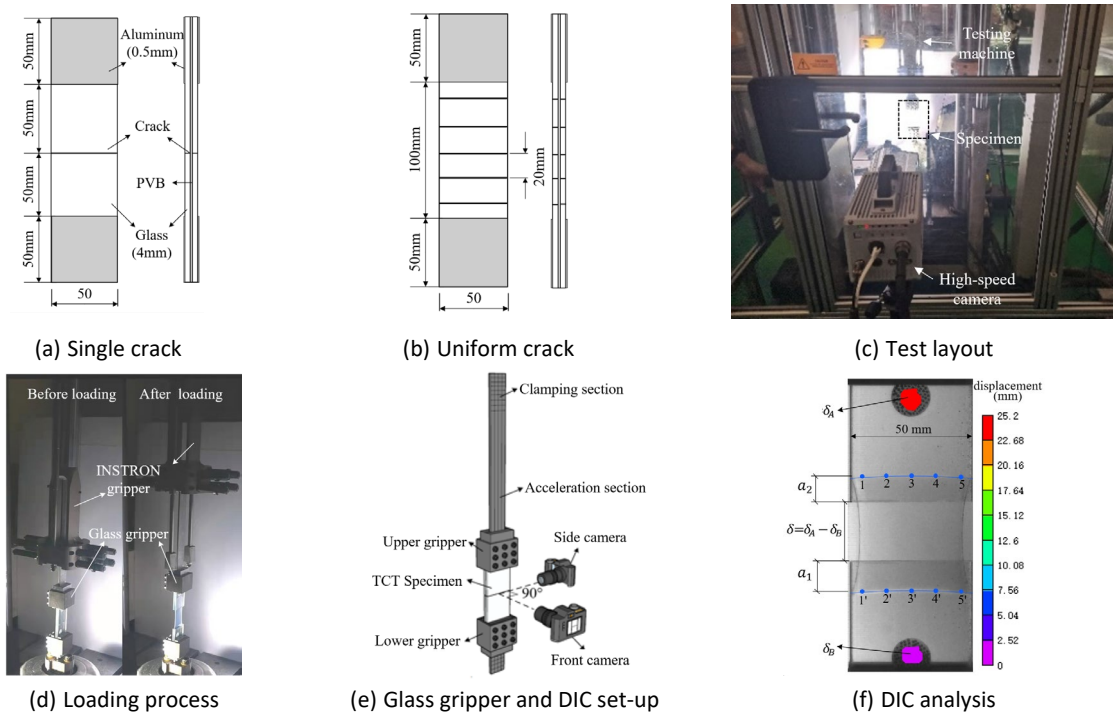
Fig. 2: TCT test.

The specimens were labelled in form of "A-B-C-D," in which A represents the interlayer adhesion grade (BG-R15 or BG-R20), B stands for the crack patterns (SC, short for single-crack, and MC, short for multi-cracks). C is the loading rate (0.1m/s, 0.5m/s, and 5m/s), and D indicates the specimen no.. For instance, BG-R15-SC-0.1m/s-2 represents the second BG-R15 PVB-laminated glass specimen with single crack subjected to a loading rate of 0.1m/s. The test condition is shown in Table 1.

Table 1: Summary of the TCT tests.

PVB type	Pummel value [a]	PVB thickness (mm)	Crack pattern	Loading rate (m/s)	Specimen number
BG-R15	5±2	1.52	SC, MC	0.1, 0.5, 5	3
BG-R20	≥6				

Note: a. Pummel values are from the Kuraray's product manuals (Kuraray 2017a, 2017b, and 2017c).

3.2. Delamination phenomenon

Figure 3 shows the delamination process of single-crack and multi-crack specimens at 0.5m/s loading rate. There are distinct differences of the delamination phenomenon between BG-R15 and BG-R20 laminated glass. The delamination capacity of BG-R15 is much higher than BG-R20. The BG-R15 keeps intact when the loading distance is higher than 50mm, while the maximum displacement of BG-R15 is around 3mm for single-crack and 9mm for multi-crack.

| δ = 1mm | 10mm | 30mm | 50mm |
(a) BG-R15-SC-0.5m/s-1

| δ = 1mm | 10mm | 30mm | 50mm |
(b) BG-R15-MC-0.5m/s-1

| δ = 0.1mm | 1mm | 2mm | 3mm |
(c) BG-R20-SC-0.5m/s-1

| δ = 1mm | 4mm | 6mm | 9mm |
(d) BG-R20-MC-0.5m/s-1
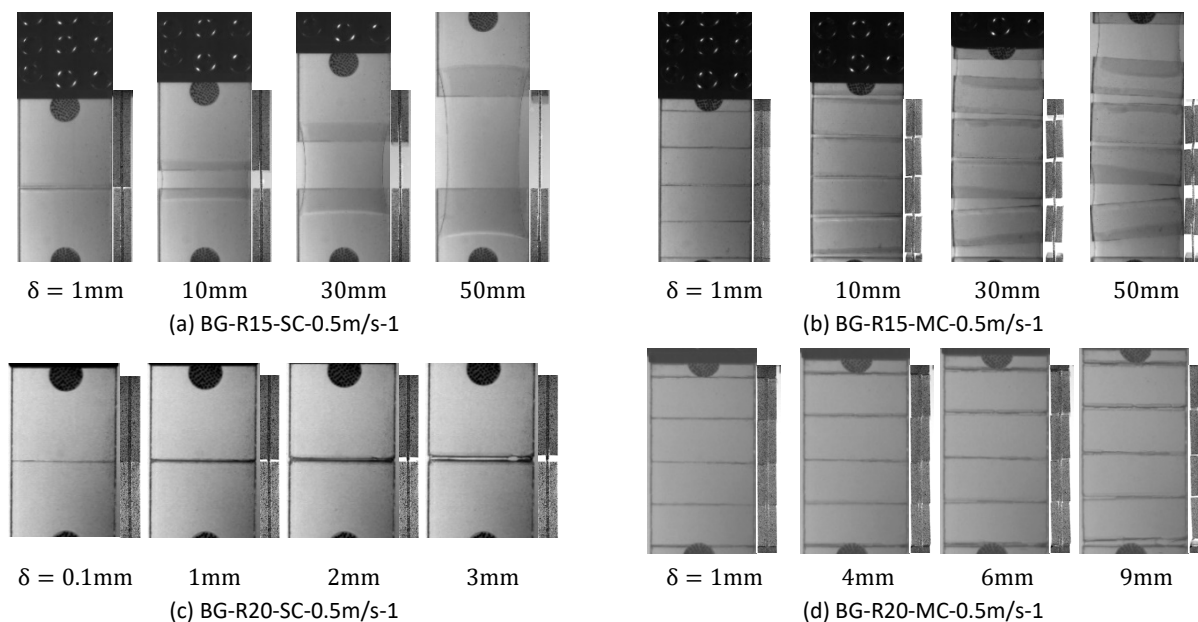
Fig. 3: TCT test phenomena.

3.3. Force/delamination-displacement curves

Figure 4 shows the obtained force-displacement (F-δ) diagrams for all specimens and delamination length-displacement (DL-δ) diagrams for single crack BG-R15 PVB-laminated glass. The delamination length of BG-R20 PVB-laminated glass is too small to be obtained accurately. The decrease in the force-displacement diagram indicates a gradually rupture of the interlayer. Obvious plateaus can be observed in the force-displacement curve for BG-R15 PVB-laminated glass, and the plateau force increases with the increase of loading rate. Besides, the force-displacement curve of single-crack specimen at 0.1 m/s is basically the same as that of the specimen with five uniformly distributed cracks at 0.5 m/s, which proves the time correlation property of the interlayer and adhesion interface. Due to the high interfacial adhesion of BG-R20 PVB-laminated glass, there is no plateau in the test curves of single-cracked specimens. The maximum displacement increases significantly with the increase of crack numbers. With the increase of loading rate, the delamination length and maximum displacement decrease significantly. The bearing capacity of BG-R20 is slightly higher than that of BG-R15, but the maximum displacement is significantly lower, indicating worse deformability.

(a) BG-R15

(b) BG-R20
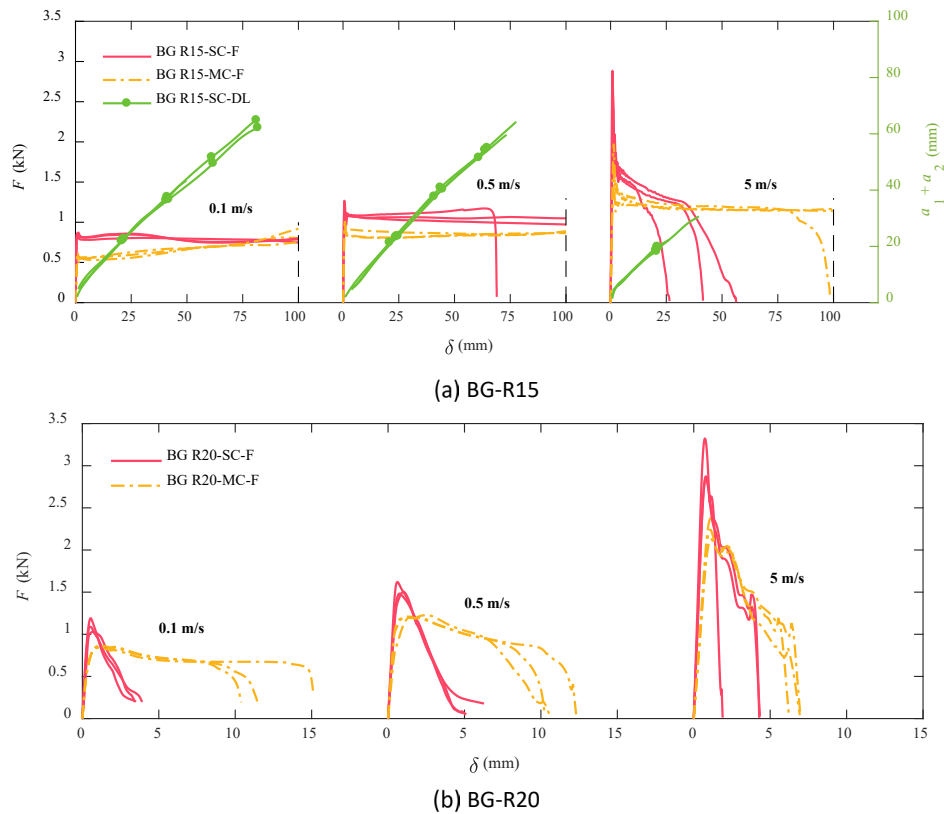
Fig. 4 Test results of force/delamination length–displacement curves.

4. Calibration of interfacial properties

4.1. Numerical model

A numerical model with cohesive elements (Chen et al. 2021a) was established to simulate the delamination process of BG-R15 PVB-laminated glass. The bonding strength and interfacial energy release rates at different loading rates were calibrated by matching the plateau force to the test results. A 1/4 2D model with symmetric boundary condition was established to enhance computing efficiency. The symmetric boundaries were applied on the central plane of PVB in both x and y directions, as shown in Figure 5. PVB and glass were simulated by plane strain element (CPE4R in ABAQUS/Explicit), and the interface was modeled by 2D cohesive elements (COH2D4). An element size of 0.1mm was used based on a preliminary mesh convergence analysis.
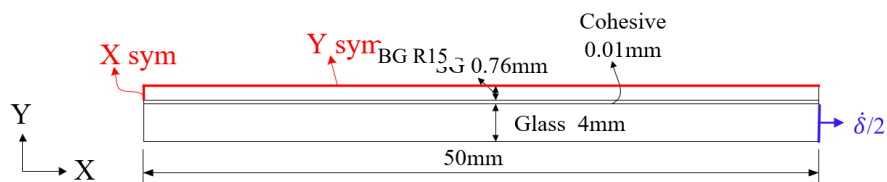
Fig. 5: 2D plane strain model and boundary conditions.

PVB is modelled as an incompressible (Poisson's ratio = 0.5) linear visco-hyperelastic material, as shown in Eq. (1) (Goh et al. 2004):

$$\sigma(\lambda, t) = \sigma_0(\lambda)g(t) \tag{1}$$

Where σ is the nominal stress, $\sigma_0(\lambda)$ is the instantaneous hyperelastic nominal stress. $g(t)$ is the viscous component of PVB material.

The first order Ogden model (Ogden 1972 and 1982) was used for the hyperelastic part of the PVB material, and the strain energy can be written as Eq. (2):

$$W = \frac{2\mu_1}{\alpha_1^2}(\lambda_1^{\alpha_1} + \lambda_2^{\alpha_1} + \lambda_3^{\alpha_1} - 3) \tag{2}$$

Where, μ_1, α_1 are material parameters, $\lambda_1, \lambda_2, \lambda_3$ are the stretches in principal directions. Under uniaxial tensile, $\lambda_1 = \lambda$, $\lambda_2 = \lambda_3 = \frac{1}{\sqrt{\lambda}}$, where λ is the stretching ratio in the loading direction.

Prony series were included to describe the viscoelastic property of PVB:

$$g(t) = g_\infty + \sum_{i=1}^{N} g_i\, e^{-t/\tau_i} \tag{3}$$

Where g_∞, g_i and τ_i are the material parameters of the Prony series. Six relaxation times τ_i ranging from 1×10^{-4} s to 10 s were considered. A genetic algorithm was applied to determine the model coefficients based on the uniaxial tensile test results. The obtained coefficients and fitting curves are shown in Figure 6a. The fitting results of the visco-hyperelastic model are in good agreement with the experimental results.

Glass is modelled as a linear elastic material. The elastic modulus, Poisson's ratio, and mass density are 72 GPa, 0.22, and 2.56 g/cm^3, respectively (Chen et al. 2021b). There is no glass fracture observed in the TCT tests so that no failure criteria were considered.

A simplified bilinear traction-separation (T-δ) law (Chen et al. 2021a) (Figure 6b) with an initial elastic response to resist crack opening followed by an irreversible damage-induced softening stage was adopted to prescribe the constitutive behaviour of the cohesive element. Three independent parameters, i.e., initial stiffness K_0, damage initiation stress σ_c, and energy release rate G_c, were defined for a given delamination mode.
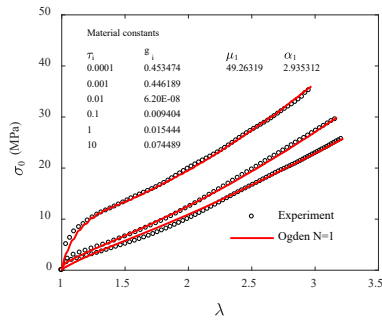
(a) Material model fit for PVB
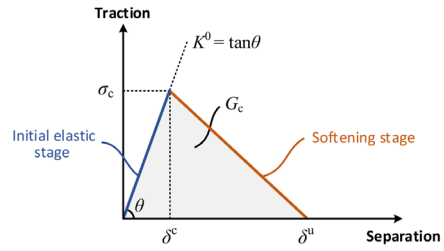
(b) Bilinear traction-separation (T-δ) law
(Chen et al. 2021a)

Fig. 6: Material properties in CZM modelling.

Figure 7 shows the numerical simulation results of BG-R15 single-crack test at 0.5m/s. The force-displacement curve and delamination length-displacement curve are in good agreement with the test results, which proves the reliability of the numerical model.
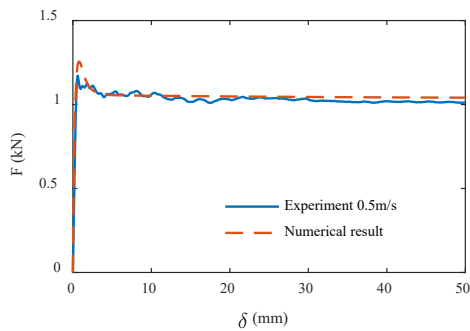
(a) Delamination phenomenon of simulation
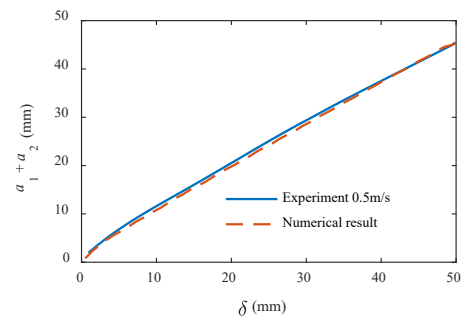
(b) Delamination length-displacement curve

Fig. 7: Numerical simulation results of BG-R15 single-crack TCT test ($\dot{\delta}$ =0.5 m/s).

4.2. Calibration of adhesion parameters

Based on a previous study by (Chen et al. 2021a), a numerical parametric analysis was conducted to calibrate the bonding strength σ_c and the energy release rate G_c for the BG-R15 laminated glass by matching the peak force (F_{peak}) and plateau force (F_{plateau}) of the simulation results to those of the tests. The results are summarized in Table 2. The simulation errors of peak force and plateau force at 5m/s are larger than 15%. A possible reason may be that the strain rate on the interlayer nearby the delamination front is 276/s for BG-R15 (Figure 8), which is much higher than the strain rate range in the material tests (Figure 1b). The material model shows good accuracy within a strain rate range from 1/s to 120/s, but gives poor prediction when extrapolated to higher strain rate. Based on the results, it can be concluded that the bonding strength σ_c and energy release rate G_c of BG-R15 PVB shows a significant rate effect. The results corresponding to specimens with multi-cracks is believed to be more reliable since more cracks can help minimize the discrepancy between specimens. Based on the results of BG-R15 PVB-laminated glass with multi-cracks, the bonding strength and energy release rate increase by nearly 25% and 50%, respectively, as the loading rate increases from 0.1m/s to 5m/s. As a result, the energy required to delaminate interface with a certain area increases with increasing

loading rate. This could be another reason for a higher overall energy dissipation of cracked PVB-laminated glass at higher loading rate, apart from the strain rate sensitivity of PVB itself.

Table 2: Comparison of the results from the numerical simulations and the tests.

Adhesion level	Crack pattern	Loading rate (m/s)	σ_c (MPa)	G_c (mJ/mm²)	F_{peak} (kN)			$F_{plateau}$ (kN)		
					test	FEA	error (%)	test	FEA	error (%)
BG-R15	Single-crack	0.1	6.5	2.1	0.86	0.87	1.16	0.81	0.80	-1.27
		0.5	7.0	2.3	1.22	1.26	3.28	1.06	1.06	0
		5	8.0	2.4	2.60	1.98	-23.85	1.42	1.64	15.49
	multi-cracks	0.1	6.0	1.6	0.58	0.59	1.72	0.56	0.56	0
		0.5	7.5	2.1	0.96	0.89	-7.29	0.84	0.84	0
		5	7.5	2.4	1.82	1.58	-13.19	1.24	1.25	0.81

Note: $F_{plateau}$ is the average force from $\delta = 5$mm to $\delta = 20$mm.
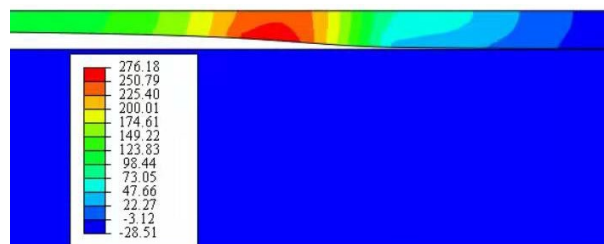
Fig. 8: Strain rate distribution nearby the delamination front of BG-R15 ($\dot{\delta} = 5$m/s).

5. Conclusion

In this paper, experimental and numerical studies are presented to investigate the interfacial properties of PVB-laminated glass. The influences of adhesion grades and loading rates are studied. The main conclusions are summarized as follows:

1. The adhesion grade dominates the delamination ability of PVB-laminated glass. The delamination length of BG-R15 PVB-laminated glass is much larger than that of BG-R20 PVB-laminated glass since higher adhesion can inhibit interfacial crack opening. Since larger delamination length brings more PVB into the overall stretch and could reduce the stress level, the BG-R15 PVB-laminated glass exhibits a lower load-bearing capacity but a higher deformability than the BG-R20 PVB-laminated glass. The deformation capacity of cracked laminated glass increases with the increase of crack number, especially for high adhesion grade laminated glass.

2. The loading rate has a significant influence on the interfacial adhesion properties of PVB-laminated glass. The energy release rates of BG-R15 at 0.1m/s, 0.5m/s, and 5m/s are 1.6, 2.1, and 2.4 mJ/mm² for multi-cracks BG-R15 PVB-laminated glass specimen, indicating a nearly 50% increase on the energy release rate as the loading rate increases. As a result, the energy dissipation due to delamination increases significantly at higher loading rate.

Acknowledgment

References

BS ISO 37, Rubber, vulcanized or thermoplastic - Determination of tensile stress-strain properties. 2017: British Standards Institute, London (2017)

Butchart C., Overend M. Delamination in fractured laminated glass [J]. Proceedings of Engineered Transparency International Conference at Glasstec, Düsseldorf, Germany. 249-257 (2012)

Chen X., Rosendahl P. L., Chen S., Schneider J. On the delamination of polyvinyl butyral laminated glass: Identification of fracture properties from numerical modelling [J]. Construction and Building Materials. 306: 124827 (2021a). https://doi.org/10.1016/j.conbuildmat.2021.124827

Chen X., Chen S., Li G. Experimental investigation on the blast resistance of framed PVB-laminated glass[J]. International Journal of Impact Engineering. 149: 103788 (2021b). https://doi.org/10.1016/j.ijimpeng.2020.103788

Chen X., Schuster M., Schneider J. On the Pummel Test and Pummel-Value Evaluation of Polyvinyl Butyral Laminated Safety Glass Composite Structures. 280(1), 114878 (2022). https://doi.org/10.1016/j.compstruct.2021.114878

Del Linz P., Hooper P. A., Arora H., Wang Y., Smith D., Blackman B. R. K., et al. Delamination properties of laminated glass windows subject to blast loading [J]. International Journal of Impact Engineering. 105: 39-53 (2017). https://doi.org/10.1016/j.ijimpeng.2016.05.015

Delincé D., Callewaert D., Belis J., Impe R., Galmart F., Matthijs N. Influence of Temperature on Post-Breakage Behaviour of Laminated Glass Beams : Experimental Approach [C]. Challenging Glass 2 – Conference on Architectural and Structural Applications of Glass, TU Delft. 407-414 (2010)

Elzière P., Dalle-Ferrier C., Barthel E., Creton C., Ciccotti M. Large strain viscoelastic dissipation during interfacial rupture in laminated glass [J]. Soft Matter. 13(08) (2017). https://doi.org/10.1039/c6sm02785g

Ferretti D., Rossi M., Royer-Carfagni G. Through-cracked tensile delamination tests with photoelastic measurements [C]. Challenging Glass 3: Conference on Architectural and Structural Applications of Glass, TU Delft. 641-652 (2012).

Fourton P., Piroird K., Ciccotti M., Barthel E. Adhesion rupture in laminated glass: influence of adhesion on the energy dissipation mechanisms [J]. Glass Structures & Engineering. 5(03): 397-410 (2020). https://doi.org/10.1007/s40940-020-00136-4

Franz J., Schneider J., Kuntsche J., Hilcken J. Untersuchungen zum Resttragverhalten von Verbundglas: Through-Cracked-Tensile Test.: John Wiley & Sons, Ltd, (2014). https://doi.org/10.1002/9783433604557.ch20

Goh S., Charalambides M., Williams J. Determination of the Constitutive Constants of Non-Linear Viscoelastic Materials [J]. Mechanics of time-dependent materials. 8(3): 255-268 (2004). DOI:10.1023/B:MTDM.0000046750.65395.FE

Kuraray. Specification Trosifol Clear B100 LR (TROSIFOL BG R10 0.76mm Clear). Tokyo, Japan: Kuraray Co. Ltd. (2017a)

Kuraray. Specification Trosifol Clear B100 MR (TROSIFOL BG R15 0.38 mm 2.28 mm). Tokyo, Japan: Kuraray Co. Ltd. (2017b)

Kuraray. Specification Trosifol Clear B100 NR (TROSIFOL BG R20 0.76 mm 1.52 mm). Tokyo, Japan: Kuraray Co. Ltd. (2017c)

Muralidhar S., Jagota A., Bennison S. J., Saigal S. Mechanical behaviour in tension of cracked glass bridged by an elastomeric ligament [J]. Acta Materialia. 48(18): 4577-4588 (2000). https://doi.org/10.1016/s1359-6454(00)00244-5

Ogden R. W. Large Deformation Isotropic Elasticity: On the Correlation of Theory and Experiment for Compressible Rubberlike Solids [J]. Proceedings of the Royal Society of London A Mathematical and Physical Sciences. 326(1567): 565-584 (1972). https://doi.org/10.1098/rspa.1972.0096

Ogden R. W. Elastic Deformations of Rubberlike Solids [M]. HOPKINS H G, SEWELL M J. Mechanics of Solids. Oxford; Pergamon. 499-537 (1982). https://doi.org/10.1016/b978-0-08-025443-2.50021-5

Samieian M. A., Cormie D., Smith D., Wholey W., Blackman B. R. K., Dear J. P., et al. Temperature effects on laminated glass at high rate [J]. International Journal of Impact Engineering. 111: 177-186 (2018). https://doi.org/10.1016/j.ijimpeng.2017.09.001

Samieian M. A., Cormie D., Smith D., Wholey W., Blackman B. R. K., Dear J. P., et al. On the bonding between glass and PVB in laminated glass. Engineering Fracture Mechanics. 214: 504-519 (2019). https://doi.org/10.1016/j.engfracmech.2019.04.006

Schuster M., Schneider J., Nguyen T. A. Investigations on the execution and evaluation of the Pummel test for polyvinyl butyral based interlayers [J]. Glass Structures & Engineering. 5(03): 371-396 (2020). https://doi.org/10.1007/s40940-020-00120-y

Sha Y., Hui C. Y., Kramer E. J., Garrett P. D., Knapczyk J. W. Analysis of adhesion and interface deadhesion in laminated safety glass [J]. Journal of Adhesion Science and Technology. 11(01): 49-63 (1997). https://doi.org/10.1163/156856197x01010

VIC-2D_Testing_Guide. West Columbia: Correlated Solutions, Inc. (2021)

Yang J., Wang Y., Wang X., Hou X., Zhao C., Ye J. Local bridging effect of fractured laminated glass with EVA based hybrid interlayers under weathering actions [J]. Construction and Building Materials. 314: 125595 (2022). https://doi.org/10.1016/j.conbuildmat.2021.125595

Platinum Sponsor

Gold Sponsors

Silver Sponsors

Organising Partners